

# FAR: A General Framework for Attributional Robustness

Adam Ivankay<sup>1,2</sup>, Ivan Girardi<sup>1</sup>, Chiara Marchiori<sup>1</sup>, Pascal Frossard<sup>2</sup>

<sup>1</sup> IBM Research Zürich

<sup>2</sup> École Polytechnique Fédérale de Lausanne (EPFL)

aiv@zurich.ibm.com, ivg@zurich.ibm.com, chi@zurich.ibm.com, pascal.frossard@epfl.ch

## Abstract

Attribution maps have gained popularity as tools for explaining neural networks' predictions. By assigning an importance value to each input dimension that represents their influence towards the outcome, they give an intuitive explanation of the decision process. However, recent work has discovered vulnerability of these maps to imperceptible, carefully crafted changes in the input that lead to significantly different attributions, rendering them meaningless. By borrowing notions of traditional adversarial training - a method to achieve robust predictions - we propose a novel *framework for attributional robustness* (FAR) to mitigate this vulnerability. Central assumption is that similar inputs should yield similar attribution maps, while keeping the prediction of the network constant. Specifically, we define a new generic regularization term and training objective that minimizes the maximal dissimilarity of attribution maps in a local neighbourhood of the input. We then show how current state-of-the-art methods can be recovered through principled instantiations of these objectives. Moreover, we propose two new training methods, *AAT* and *AdvAAT*, derived from the framework, that directly optimize for robust attributions and predictions. We showcase the effectivity of our training methods by comparing them to current state-of-the-art attributional robustness approaches on widely used vision datasets. Experiments show that they perform better or comparably to current methods in terms of attributional robustness, while being applicable to any attribution method and input data domain. We finally show that our methods mitigate undesired dependencies of attributional robustness and some training and estimation parameters, which seem to critically affect other methods.

## Introduction

Undoubtedly, the prediction performance of deep neural networks (DNNs) has been increasing in recent years. As networks become larger and deeper, their complexity also increases. This makes it difficult for humans to understand and reason about their decision process. Therefore, methods that provide insight and reason about the prediction outcome of DNNs are crucial for successfully deploying these complex networks in real-life scenarios. A recent trend in interpreting the decision process of DNNs has been to use *attribution maps* as explanations. These assign an importance value to each input dimension that represents

its *influence* on the outcome of the decision. While these methods are fast to compute (a few forward and backward passes of the network), they do not require specific domain knowledge to give interpretable explanations - *the outcome is the given class because of the salient region in the input*, hence their popularity. Most of these methods, like Saliency (Simonyan, Vedaldi, and Zisserman 2013), Integrated Gradients (Sundararajan, Taly, and Yan 2017), SmoothGrad (Smilkov et al. 2017) or DeepLIFT (Shrikumar, Greenside, and Kundaje 2017) utilize the input gradient of the network to construct the attribution map, giving explanation on the networks behaviour in a region around the given input. However, the authors in (Ghorbani, Abid, and Zou 2019) have successfully demonstrated that these explanations can be adversarially manipulated by adding carefully crafted perturbations to the input, fundamentally changing the attributions. This is especially problematic in high-stake or safety critical scenarios, where the decision outcome needs to be accompanied by a sound explanation. Attackers could willingly manipulate the salient region in a pathology image, critically misleading the medical professional assessing the decision. In other instances, they could induce false bias in automatic credit scoring algorithms by pointing to the individuals race as reason for a low score. These are critical aspects that prevent DNNs from being adopted to solve real life problems. Therefore, it is crucial for attribution maps to be robust in the local neighbourhood of the input and resistant against adversarial manipulations. Figure 1 exemplifies the adversarial fragility of attribution maps.

**Our contributions.** Even though attributional fragility is a newly discovered phenomenon, there have already been efforts to improve robustness of attribution maps. These works mostly connect robust attributions to robust predictions and adversarial robustness (Etman et al. 2019; Singh et al. 2019). However, there is no general method applicable on a wide range of attribution maps. Moreover, they do not allow for independently assessing the problem of robust explanations - with no regard for adversarial robustness in prediction. Therefore, we propose a novel *framework for attributional robustness* (FAR) as means to increase the robustness of attribution maps. It follows the premise that visually indistinguishable inputs should give near-identical attributions while maintaining the infer-

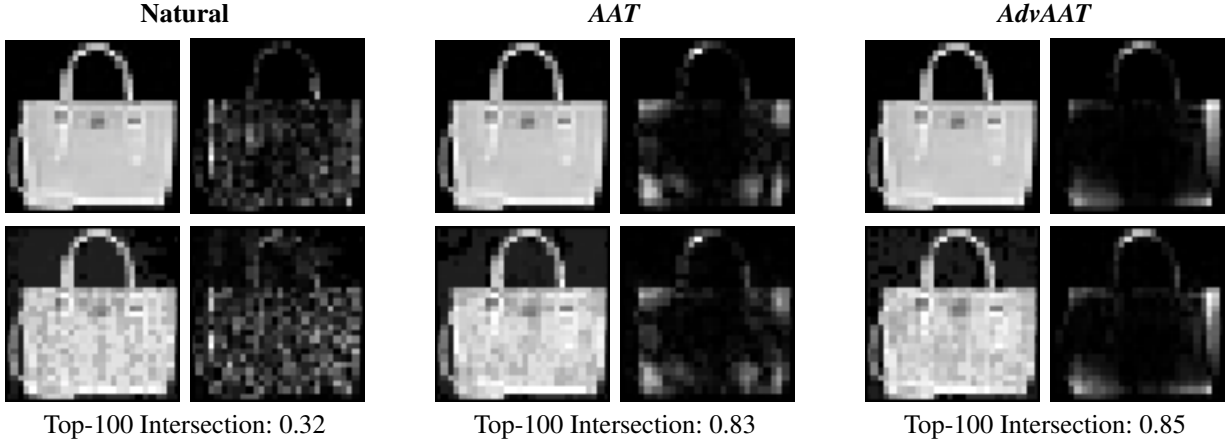


Figure 1: Integrated Gradients (IG) and their attacked saliency maps of the natural model (left), our AAT (middle) and our AdvAAT (right) method, trained on Fashion-MNIST. For each model, the upper row contains the unperturbed image in the left column and its IG saliency map in the right column, the lower row contains the corresponding perturbed image on the left and the resulting adversarial IG saliency map on the right. In each case, the networks give the correct prediction. The attribution maps of models trained by our methods seem less noisy and are more robust to perturbations (measured by the intersection ratio of the 100 pixels with largest attributions in the unperturbed and the adversarial attribution map - *Top-100 intersection*).

ence output unchanged, extending the idea of traditional adversarial training described in (Madry et al. 2017). In contrary to other approaches, our framework allows sole optimization for robust attributions as well as combining robust prediction with robust attribution, two crucial properties of trustworthy and explainable deep neural networks. It comprises two generic training objectives that enable robustification of any differentiable saliency map in terms of any differentiable attribution dissimilarity metric. We show that three current robust attribution techniques are principled instances of this framework. Then, we propose two new instantiations of FAR, our AAT and AdvAAT methods that directly optimize for maximal correlation between original and adversarial feature importance, encouraging the ranking of input features to be similar within a small  $L_\infty$  neighbourhood of the input. Experiments on MNIST (LeCun 1998), Fashion-MNIST (Xiao, Rasul, and Vollgraf 2017), CIFAR-10 (Krizhevsky 2009) and GTSRB (Stallkamp et al. 2011) show that models trained with AAT and AdvAAT give more robust attribution maps than current existing methods for MNIST and Fashion-MNIST, and comparably robust maps on CIFAR-10 and GTSRB. Lastly, we identify that gradient-based attribution maps can have undesired dependencies on the weight initialization of the network (even for adversarially trained networks) and on the tightness parameter of the ReLU approximations. Our AAT method mitigates these dependencies, yet we stress the need for detailed reporting and assessment of other parameter dependencies in a diverse evaluation setup.

### Preliminaries

**Background.** Let  $f_t(\mathbf{x})$  be a DNN with prediction  $y = \arg \max_t f_t(\mathbf{x})$  and input gradient  $g_t^x(\mathbf{x})$  for class  $y$ . An **attribution method**  $S(\mathbf{x}, f, \cdot)$  is a function that assigns an

importance value to each element of  $\mathbf{x}$  towards the decision of DNN  $f_t(\mathbf{x})$ .

The simplest attribution map considered in this work is the **Saliency Map** (SM) defined as follows:

$$S(\mathbf{x}, f) = \nabla_{\mathbf{x}} f_t(\mathbf{x}) := |g_t^x(\mathbf{x})| \quad (1)$$

An axiomatic approach to attribution is **Integrated Gradients** (IG), which is a smoothed version of SM (Sundararajan, Taly, and Yan 2017). IG is defined in Equation (2) and fulfills the *completeness axiom* written in Equation (3).

$$S(\mathbf{x}, f, \mathbf{b}) = (\mathbf{x} - \mathbf{b}) \cdot \int_{\alpha=0}^1 \nabla_{\mathbf{x}} f_t(\tilde{\mathbf{x}})|_{\tilde{\mathbf{x}}=\mathbf{b}+\alpha(\mathbf{x}-\mathbf{b})} d\alpha \quad (2)$$

$$\sum_{i \in d} S(\mathbf{x}, f, \mathbf{b})_i = f_t(\mathbf{x}) - f_t(\mathbf{b}) \quad (3)$$

where  $d$  denotes the dimensionality of input  $\mathbf{x}$ .

While SM provides an intuition on how the prediction would change in the *locality* of the input, it fails to fulfill certain axioms for good explanations. However, IG is a principled approach that fulfills sensitivity, implementation invariance and completeness axioms (Sundararajan, Taly, and Yan 2017), which makes it a commonly accepted and used explanation method.

**Attributional robustness** (AR) refers to explanations' resistance towards adversarial perturbations. While there is no uniformly agreed on definition for AR, most mathematical formulations build towards the conjecture that attribution maps should be similar for similar inputs. We define AR as written in Equation (4).

$$r[S(\cdot), S_t(\cdot), f] = 1 - \max_{\tilde{\mathbf{x}}} d_s[S(\tilde{\mathbf{x}}, f, \cdot), S_t(\cdot)] \quad (4)$$

with  $\|\mathbf{x} - \tilde{\mathbf{x}}\|_p < \varepsilon$  and  $\arg \max_t f_t(\mathbf{x}) = \arg \max_t f_t(\tilde{\mathbf{x}})$ .  $r[S(\cdot), S_t(\cdot), f]$  denotes the attributional robustness of

saliency map  $S(\cdot)$ , target saliency map  $S_t(\cdot)$  and classifier  $f$ ,  $\tilde{\mathbf{x}}$  and  $\mathbf{x}$  the adversarial and original input,  $\varepsilon$  a small bound on the  $p$ -norm of the input change, and  $d_s(\cdot)$  denotes a (scaled) dissimilarity metric for attribution maps.

**Related work.** The phenomenon of fragile attribution maps was discovered by the authors of (Ghorbani, Abid, and Zou 2019). They used an iterative feature importance attack (IFIA, Algorithm 1), inspired by the Projected Gradient Descent (PGD) attack from the authors of (Madry et al. 2017) on predictions, to maximize the dissimilarity between adversarial and original attribution maps, while keeping the prediction of the network unchanged. The authors suggest the *Sum-of-Top-K*, *Mass-Center* and *Targeted* dissimilarity functions. We refer to the original paper for the definitions. Algorithm 1 contains the pseudocode for the attack. The authors of (Dombrowski et al. 2019) added an additional term to penalize class probability differences as well.

First efforts for mitigating attributional fragility were introduced in (Etmann et al. 2019). The authors proved theoretical connections between adversarial robustness and the *alignment*  $\langle g_t^x(\mathbf{x}), \mathbf{x} \rangle$  of class input gradients  $g_t^x(\mathbf{x})$  and input  $\mathbf{x}$ . Based on this consideration, it has been shown that adversarially trained networks (in their predictions) have increased attributional robustness (Chen et al. 2019; Singh et al. 2019; Wang et al. 2020). On the other side, the authors of (Singh et al. 2019) have achieved state-of-the-art AR by maximizing alignment with a regularization term during training. However, the input-gradient alignment as an upper bound for robustness strictly only holds in a local linear neighbourhood of input. Moreover, it depends on both the input and its gradients, as it computes the inner product between them. This is a strong assumption, as zero-input areas do not contribute to the alignment, no matter their gradient.

A different, axiomatic approach to robust saliency maps has been introduced in (Chen et al. 2019). The authors utilize Integrated Gradients (IG) (Sundararajan, Taly, and Yan 2017) and its theoretical properties to attain robust attributions. Therefore, the method is only suitable for robustifying gradient-based attributions, while simultaneously reaching robust predictions as well. In other research, the works of (Dombrowski et al. 2019) and (Wang et al. 2020) analyzed the local geometry of the classifier, effectively reducing attribution fragility by smoothing the curvature of the classifier. This is consistent with previous observations of correlations between adversarially robust networks and robust attributions (Etmann et al. 2019; Singh et al. 2019). While there has been significant effort in mitigating adversarial vulnerability of attribution maps, no method is suitable for a wide range of saliency algorithms - not only gradient-based ones. Additionally, none allow for directly optimizing for similar attributions and studying the influences of robust saliencies on adversarial robustness.

## Framework for Attributional Robustness

In this section, we introduce FAR, our framework to robustify attribution maps in DNNs. It consists of two generic training objectives for robust attributions as well as predic-

---

### Algorithm 1: Iterative feature importance attack

---

**Input:** Classifier  $f$ , input  $\mathbf{x}$ , target class  $t$ , attribution map  $S(\cdot)$ , dissimilarity metric  $d$ , norm  $p$  and bound  $\varepsilon$ , step size  $\eta$ , iterations  $N$ , data bounds  $k$

**Output:** Adversarial example  $\mathbf{x}_{\text{adv}}$

```

 $\mathbf{x}_{\text{adv}} \leftarrow \mathbf{x};$ 
while  $i < N$  and
   $\arg \max_t f_t(\mathbf{x}_{\text{adv}}) = \arg \max_t f_t(\mathbf{x})$  do
     $\mathbf{g}_t \leftarrow \nabla_{\mathbf{x}_{\text{adv}}} d[S(\mathbf{x}_{\text{adv}}, f, \cdot), S(\mathbf{x}, f, \cdot)];$ 
     $\mathbf{e}_t \leftarrow \text{Normalize}_p[\mathbf{g}_t];$ 
     $\mathbf{x}_{\text{adv}} \leftarrow \mathbf{x}_{\text{adv}} + \eta \mathbf{e}_t;$ 
     $\mathbf{x}_{\text{adv}} \leftarrow \text{Project}_p[\mathbf{x}_{\text{adv}}, \mathbf{x}, \varepsilon, k]$ 
end

```

---

tions. Then, we show how existing robust attribution objectives can be derived from these objectives.

We want to stress three shortcomings of current AR methods. First, they jointly optimize for both adversarial and attributional robustness. This does not allow for a separate analysis of the two notions. Second, the authors of both (Chen et al. 2019) and (Singh et al. 2019) base their methods on gradient-based attribution maps. It is not straightforward to adapt them to non-differentiable attributions. Third, state-of-the-art methods do not directly optimize for maximizing AR, but achieve it implicitly by gradient regularization.

To mitigate these shortcomings, we extend the classical notion of adversarial training (Madry et al. 2017) to attribution maps with the premise that close to identical inputs to the DNNs should yield similar outputs - *both logits and attribution maps*. In order to formalize this, the following considerations have to be made:

- *Perceptually identical inputs.* Similarly to adversarial examples, a distance metric between inputs is required, of which it can be assumed that if bounded, the ground truth label of the data does not change.  $L_p$ -norms with small bounds  $\varepsilon$  are suitable to fulfill this requirement.
- *Similar attribution maps.* Comparing attribution maps is not straightforward. Unlike in the case of input data, it is harder to justify  $L_p$ -norms as distance metrics, as it is often argued that not all input features, but only a certain subset matter, even, only their relative ranks. Therefore, AR is determined by metrics reflecting these considerations, like *Kendall's rank order correlation* (CO) (Kendall 1938) or the *Top-K intersection* (IN) (Ghorbani, Abid, and Zou 2019).
- *Target attributions and identical prediction outcomes.* Ground truth for attribution maps is usually not available, unlike target classes in traditional adversarial training, and can be subject to interpretation. Therefore, we use the attributions of the unperturbed inputs as target attributions. Further, during the estimation of robustness, we only require the same predicted class  $\arg \max_t f_t(\mathbf{x}) = \arg \max_t f_t(\mathbf{x}_{\text{adv}})$  of original and perturbed inputs, without adding an additional term to the attack loss that penal-

izes output probability differences, as done in the work of (Dombrowski et al. 2019).

Given the above points, we define our framework as a *regularization term* and a *robust training loss*, which formulate generic objectives for robustifying any attribution method in terms of any dissimilarity. These terms are defined in the following two Equations (5) and (6).

$$R(\mathbf{x}, f, S, \cdot) = \max_{\|\tilde{\mathbf{x}} - \mathbf{x}\|_p < \varepsilon} d[S(\tilde{\mathbf{x}}, f, \cdot), S_t(\mathbf{x}, f, \cdot)] \quad (5)$$

$$L(\mathbf{x}, f, y, S, \cdot) = \max_{\|\tilde{\mathbf{x}} - \mathbf{x}\|_p < \varepsilon} \{ l(\tilde{\mathbf{x}}, y, f) + \gamma \cdot d[S(\tilde{\mathbf{x}}, f, \cdot), S_t(\mathbf{x}, f, \cdot)] \} \quad (6)$$

$R(\cdot)$  and  $L(\cdot)$  denote the training terms,  $f$  the classifier,  $l(\cdot)$  the classification loss,  $d(\cdot)$  is any smooth dissimilarity metric between saliency map  $S(\cdot)$  and a target attribution  $S_t(\cdot)$ ,  $p$  denoting an  $\varepsilon$ -bounded norm base and  $y$  the target class. The rest of the notation is kept from the previous sections. Using these terms, the general training objectives become the following *min-max* optimization problems written in Equations (7) and (8).

$$\theta^* = \arg \min_{\theta} \sum_{\mathbf{x} \sim D} \{ l(\mathbf{x}, y, f) + \lambda R(\mathbf{x}, f, S, \cdot) \} \quad (7)$$

$$\theta^* = \arg \min_{\theta} \sum_{\mathbf{x} \sim D} L(\mathbf{x}, f, y, S, \cdot) \quad (8)$$

with notation defined as in previous sections. Note that while Equation (7) allows for solely optimizing for robust attributions, the training loss described in Equation (8) encourages both robust attributions *and* predictions, controlled by the parameter  $\gamma$ .

We would like to stress the following advantages of formulating the AR problem as above. First, the choice of  $S(\cdot)$  is not fixed - the framework can be used to robustify any saliency map. However, for non-differentiable methods, an estimation of input gradients is needed. Second, the dissimilarity metric  $d(\cdot)$  can be chosen arbitrarily, depending on the requirements of the use case. As previously mentioned, robustness in attributions can be defined in several ways. Our framework allows for optimizing for any subdifferentiable  $d(\cdot)$ . Third, by varying the regularization parameters, we can adjust the trade-off between optimizing for robust attributions and predictions.

**Recovering existing objectives.** In this section, we demonstrate that current existing robustness objectives can be recovered by principled instantiations of the previously introduced framework.

**Madry’s Robust Prediction** (Madry et al. 2017) can be recovered by setting  $\gamma = 0$  and using the optimization term written in Equation (6) with Equation (8). The summation term including  $S(\cdot)$  will be zero and the Objective results as follows:

$$\theta^* = \arg \min_{\theta} \sum_{\mathbf{x} \sim D} \max_{\|\tilde{\mathbf{x}} - \mathbf{x}\|_p < \varepsilon} l(\tilde{\mathbf{x}}, y, f) \quad (9)$$

The **Axiomatic Attribution Regularization** (IG-NORM and IG-SUM-NORM) terms in (Chen et al. 2019) can be recovered using the regularization term in Equation (5) with the IG attribution map  $S(\mathbf{x}_{adv}, f, \mathbf{b}) = \mathbf{IG}(\mathbf{x}_{adv}, \mathbf{b})$  with baseline  $\mathbf{b} = \mathbf{x}$  and dissimilarity function  $d = \|\cdot\|_1$ . Equation (7) then becomes as follows.

$$\theta^* = \arg \min_{\theta} \sum_{\mathbf{x} \sim D} \{ l(\mathbf{x}, y, f) + \lambda \cdot \max_{\|\tilde{\mathbf{x}} - \mathbf{x}\|_p < \varepsilon} \mathbf{IG}(\tilde{\mathbf{x}}, \mathbf{x}) \} \quad (10)$$

The IG-SUM-NORM training objective in (Chen et al. 2019) can be analogously derived from Equation (8). Note that  $S_t(\mathbf{x}, f, \mathbf{b} = \mathbf{x}) = \mathbf{IG}(\mathbf{x}, \mathbf{x}) = 0$ . Due to the completeness axiom in Equation (3), this objective also bounds the maximal change in logits for the given class,  $f(\mathbf{x}_{adv}) - f(\mathbf{x}) = \sum \mathbf{IG}(\mathbf{x}_{adv}, \mathbf{x}) \leq \sum |\mathbf{IG}(\mathbf{x}_{adv}, \mathbf{x})| = \|\mathbf{IG}(\mathbf{x}_{adv}, \mathbf{x})\|_1$ .

The input-gradient **Spatial Alignment** regularization term introduced in (Singh et al. 2019) corresponds to utilizing the sum of positive spatial alignment of true class input gradients and the negative spatial alignment of the second largest logits input gradient as attribution map  $S(\mathbf{x}, f, \cdot)$ . This is detailed in the following Equation (11):

$$S(\mathbf{x}, f, y, \bar{y}) = \cos\_sim[\nabla_{\mathbf{x}} f^y(\mathbf{x}), \mathbf{x}] - \cos\_sim[\nabla_{\mathbf{x}} f^{\bar{y}}(\mathbf{x}), \mathbf{x}] \quad (11)$$

$\cos\_sim(\cdot)$  denotes the *pointwise* cosine similarity between the input gradient and the image.  $\bar{y}$  is the second largest class’ logit, the rest of the notation is kept from previous sections. By setting the dissimilarity function  $d(\cdot) = \log \{ 1 + \exp [ - \text{sum}(\cdot) ] \}$ , the regularization term in (Singh et al. 2019) can be recovered from Equation (5).

## Attributional Adversarial Training

Next, we introduce *AAT* and *AdvAAT*, our instantiations of the aforementioned FAR that achieve robust attribution maps through optimizing for maximal correlation of explanations within a small local neighbourhood of the input.

Utilizing the above described framework, we formalize the **adversarial attributional training** objectives, consisting of a *regularization term* (*AAT*) that optimizes directly for robust attributions, and a *robust training loss* (*AdvAAT*) used to achieve both robust predictions and attributions. We aim to define an objective that is a close proxy of the true attributional robustness as defined in the previous section. Therefore, as attribution maps, we choose the aforementioned IG, as it is a widely accepted axiomatic attribution method. It is not possible to optimize for the *Top-K intersection* or *Kendall’s rank order correlation* dissimilarities directly, as they utilize non-differentiable rank information. Therefore, we choose the *Pearson correlation coefficient* (Pearson 1895) loss as dissimilarity, in order to keep the ranking of features constant. This leads to the following optimization

regularization term (12) and loss (13) respectively.

$$\theta_{\text{AAT}}^* = \arg \min_{\theta} \sum_{\mathbf{x} \sim \mathcal{D}} \left\{ l(\mathbf{x}, y, f) + \lambda \max_{\|\tilde{\mathbf{x}} - \mathbf{x}\|_{\infty} < \varepsilon} \text{PCL}[\text{IG}(\tilde{\mathbf{x}}, \mathbf{b}), \text{IG}(\mathbf{x}, \mathbf{b})] \right\} \quad (12)$$

$$\theta_{\text{AdvAAT}}^* = \arg \min_{\theta} \sum_{\mathbf{x} \sim \mathcal{D}} \max_{\|\tilde{\mathbf{x}} - \mathbf{x}\|_{\infty} < \varepsilon} \left\{ l(\tilde{\mathbf{x}}, y, f) + \gamma \cdot \text{PCL}[\text{IG}(\tilde{\mathbf{x}}, \mathbf{b}), \text{IG}(\mathbf{x}, \mathbf{b})] \right\} \quad (13)$$

with  $\text{PCL}(\cdot) = 1 - [\text{PCC}(\cdot) + 1]/2$  denoting the loss derived from *Pearson correlation coefficient*  $\text{PCC}(\cdot)$ .  $\mathcal{D}$  denotes the data distribution,  $\theta^*$  the optimal parameters of the classifier,  $l(\cdot)$  the cross-entropy classification loss and  $\text{IG}(\cdot, \mathbf{b})$  the IG attribution with baseline  $\mathbf{b} = \mathbf{0}$ .  $\tilde{\mathbf{x}}$  and  $\mathbf{x}$  stand for the perturbed and unperturbed input,  $\lambda$  and  $\gamma$  are parameters that control the regularization.

The outer minimization is solved by standard gradient descent of the loss in the network parameter space. The inner maximization is estimated with the IFIA attack (Algorithm 1) described in the previous section. During this attack, we approximate the second derivative of the ReLU networks with the second derivative of the Softplus activation  $\nabla_{\mathbf{x}}^2 \text{ReLU}(\mathbf{x}) := \beta \cdot \text{sigm}(\beta \cdot \mathbf{x}) \cdot [1 - \text{sigm}(\beta \cdot \mathbf{x})]$ , where  $\text{sigm}$  is the standard sigmoid function,  $\beta$  a sharpness parameter that controls the approximation tightness of the ReLU (Dombrowski et al. 2019). As such, we decouple the attribution maps from the actual estimation of their robustness, as the first order gradients are kept as the standard derivatives of the ReLU.

## Experiments and Results

In this section, we report the experimental setup and evaluation of our *AAT* and *AdvAAT* methods. Utilizing the datasets MNIST, Fashion-MNIST, CIFAR-10 and GTSRB, we show that our methods outperform current state-of-the-art on the former two datasets and perform comparably to state-of-the-art on the latter two in terms of attributional robustness. Additionally, to our knowledge, we are the first to experimentally show the dependency of attribution robustness on the weight initialization of the networks, and argue that training with our objectives lessens these dependencies. Moreover, we show that the tightness parameter  $\beta$  in the approximation of second order ReLU gradient significantly influences the robustness estimation. We therefore conclude that care needs to be taken when using gradient-based attributions maps on naturally trained models and highlight the need for careful assessment of dependencies and a wide evaluation spectrum in future research.

**Setup.** We compare three state-of-the-art attribution robustification methods (Adv, IG-SN and Align), taken from (Madry et al. 2017), (Chen et al. 2019) and (Singh et al. 2019) respectively, and a naturally trained (Nat) models’ attributional robustness to networks trained with

our robust training objectives from Equations (7) (*AAT*) and (8) (*AdvAAT*), on the aforementioned four datasets. For MNIST and Fashion-MNIST, we train a two-layer convolutional neural network with 32 and 64 layers respectively, for CIFAR-10 and GTSRB we use a ResNet taken from (He et al. 2016). A detailed description on the architectures and the training details can be found in the supplemental appendix. We train similar architectures as in the state-of-the-art works, but due to computational constraints, it was not always possible to reproduce their results. In these cases, we indicate results taken from the papers with an asterisk (\*).

In order to evaluate the attributional robustness of each model, the IFIA attack from (Ghorbani, Abid, and Zou 2019) is used, utilizing their proposed *Top-K intersection* attack. We use the IG attribution map and report the *Top-K intersection*  $\text{IN}$  of original and adversarial attribution map as well as their *Kendall rank order correlation*  $\text{CO}$  as robustness metrics. We use  $k = 100$  for MNIST and Fashion-MNIST, and  $k = 1000$  for CIFAR-10 and GTSRB. Due to computational limitations, IG is computed with 5 approximation steps. We found this to yield good approximations while keeping computation cost low. The natural and adversarial accuracy ( $\text{NA}$  and  $\text{AA}$ ) of the models are also reported. The IFIA attack is executed for 7 steps, with a relative step size of  $1.2/7$ . We used three random starts for each image, reporting the resulting lowest robustness. The adversarial accuracy is evaluated using the PGD attack from (Madry et al. 2017), using 40 iterations. Table 1 contains the results of the comparison experiments.

**Numerical analysis.** Based on Table 1, we make the following conclusions. First, our instantiations outperform all other state-of-the-art methods on MNIST and Fashion-MNIST in terms of  $\text{IN}$ , while only falling short to IG-SN and Adv on Fashion-MNIST in  $\text{CO}$ . However, on CIFAR-10 and GTSRB, the input-gradient alignment-based method performs better than our methods. We believe the reason for this lies in the nature of the data. MNIST and Fashion-MNIST contain many black pixels. Our method provides gradient constraints even for these dimensions, whereas gradient alignment (Align) in these dimensions is inherently zero, due to pixel values. Moreover, gradient saturation further worsens optimization with gradient alignment target, because white pixels are targeted to have high gradients (in alignment terms), but small changes in these dimensions do not necessarily lead to any changes in the target logits. Therefore, robustifying gradients via alignment is less effective for MNIST and more effective on RGB datasets with fewer saturated pixels. These considerations are backed by the poor relative performance of the Align method on MNIST and Fashion-MNIST. Additionally, as described in the next section, we identify that different network weight initializations lead to different robustness estimates, which adds to the potential differences in performance of our and other reported methods. An extensive study on the best possible parameter combination of our methods is not part of this study, due to computational limitations.

Our second conclusion comes from comparing the *AAT*

Dataset	Model	NA	AA	IN	CO
MNIST	Nat	99.1%	0.0%	0.42	0.35
	Adv	99.0%	93.9%	0.35	0.05
	Align	98.7%	2.6%	0.52	0.40
	IG-SN	98.3%*	88.2%*	0.72*	0.31*
	AAT	98.9%	8.7%	<b>0.79</b>	<b>0.48</b>
	AdvAAT	98.6%	77.1%	0.75	<b>0.48</b>
Fashion-MNIST	Nat	90.8%	0.0%	0.32	0.42
	Adv	89.1%	70.1%	0.61	0.66
	Align	90.2%	30.5%	0.48	0.60
	IG-SN	85.4%*	70.3%*	0.72*	<b>0.67*</b>
	AAT	88.0%	18.6%	0.74	0.61
	AdvAAT	87.8%	56.5%	<b>0.76</b>	0.63
CIFAR-10	Nat	83.8%	1.8%	0.65	0.63
	Adv	64.4%	35.2%	0.80	0.78
	Align	89.8%*	37.6%*	<b>0.93*</b>	<b>0.92*</b>
	IG-SN	-	-	-	-
	AAT	68.5%	4.8%	0.81	0.76
	AdvAAT	64.0%	24.8%	0.86	0.81
GTSRB	Nat	95.8%	25.7%	0.62	0.65
	Adv	97.6%*	83.2%*	0.69*	0.75*
	Align	98.5%*	84.7%*	<b>0.92*</b>	<b>0.89*</b>
	IG-SN	95.7%*	77.1%*	0.74*	0.77*
	AAT	95.6%	26.9%	0.75	0.79
	AdvAAT	91.7%	65.9%	0.84	0.80

Table 1: Estimated attributional robustness (IN and CO) of the models trained naturally (Nat), adversarially (Adv), *alignment*-based (Align) (Singh et al. 2019), IG-SUM-NORM-based (IG-SN) as well as with our AAT and AdvAAT objectives. The results are reported on the MNIST, Fashion-MNIST, CIFAR-10 and GTSRB datasets. Their natural and adversarial accuracy is given in the NA and AA columns. Numbers indicated with an asterisk (\*) are taken from the respective work and not reproduced by us.

method to AdvAAT. AAT achieves slightly worse attribution robustness to AdvAAT, but significantly worse adversarial accuracy for all datasets experimented on. This leads us to believe that while adversarial robustness does increase attribution robustness, the reverse is only limitedly true. Regularizing gradient-based attribution maps does increase adversarial robustness, but only by a slight margin. We leave the theoretical analysis of this phenomenon to future work.

**Dependency on hyperparameters of the training and estimation process.** In this section, we would like to highlight two undesired dependencies of attributional robustness in DNNs. First, our experiments have shown that gradient-based attribution maps and their robustness estimates can depend on the *initialization of the weights in the network*. While resulting in nearly identical natural and adversarial accuracies, differently initialized networks yield considerably different robustness of gradient maps. We exemplify this with our natural, adversarially and AAT trained mod-

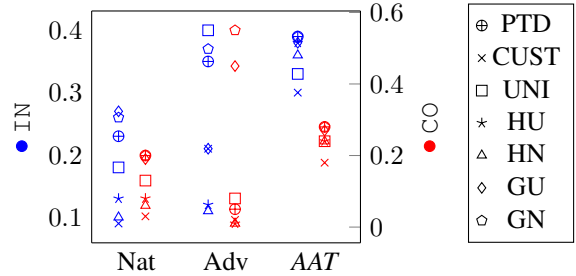


Figure 2: Estimated attributional robustness of SM (Equation 1) with *seven* different initializations for the natural (Nat), adversarially (Adv) and attributionally (AAT) trained models on MNIST. The estimated attributional robustness varies significantly for the first two models, less for the third, while keeping the training and evaluation process unchanged. The resulting accuracies of each model remain approximately the same, see further details in the supplementary appendix.

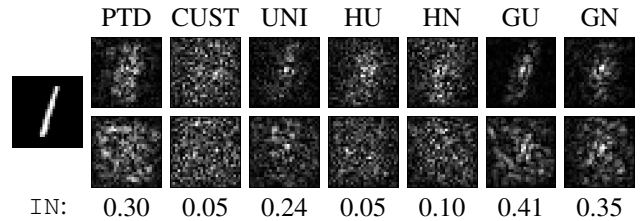


Figure 3: Gradient maps (SM) and their attacked maps of the natural model trained on MNIST for different weight initializations. The upper line contains the original SMs for each initialization, the lower line the attacked map. The initialization method affects the gradient maps, resulting in significantly different attribution robustness estimates (IN).

els on MNIST, by reporting their corresponding performance and attribution robustness estimates for seven different network weight initializations. These are the default PyTorch (Paszke et al. 2019) initialization for linear and convolutional layers (PTD), a custom initialization taken from (Chen et al. 2019) (CUST), a random uniform initialization of weights and biases with bounds  $-0.1$  and  $0.1$  (UNI) as well as the default PyTorch He (He et al. 2015) and Glorot (Glorot and Bengio 2010) uniform and normal initializations with zero bias (HU, HN and GU, GN respectively). Figure 2 reports the resulting attributional robustness estimates for the initialization methods. Both for natural and adversarially robust models, the variance of IN and CO is significant across the different initializations. The gradient maps look notably different as well, as reported in Figure 3. This dependency is partly mitigated by our method, but still present. Thus, we draw attention to the fact that even when regularizing the second gradients, the networks might still converge to different local minima with significantly different gradient maps, and comparing their robustness needs to be done with care.

The second dependency we would like to highlight is the

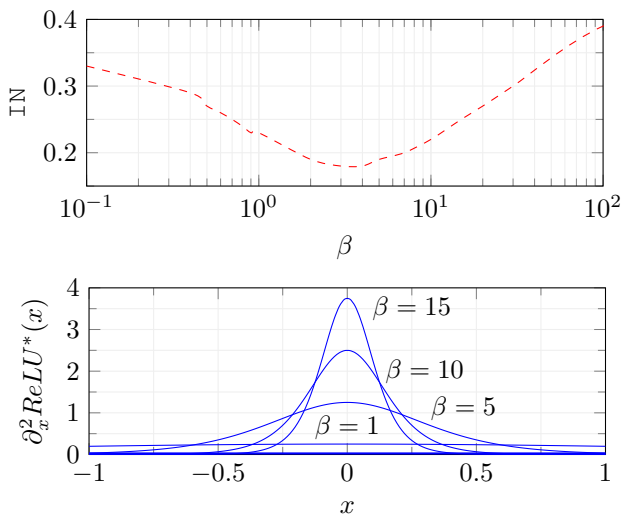


Figure 4: **Upper:** Estimated attributional robustness (IN) of SM for the natural model trained on MNIST, varying the  $\beta$  parameter of the ReLU approximation. By choosing values between 0 and 10, the estimated robustness can change significantly. **Lower:** Value of the second gradient for different  $\beta$  values. When choosing  $\beta$  too small or large, the second gradients vanish, leading to weaker robustness estimates.

**tightness parameter of the ReLU** ( $\beta$ ) second order gradient approximation. Figure 4 shows the estimated *Top-K intersection* of the natural MNIST model while using different  $\beta$  values for the second gradient approximation. We observe that by varying this parameter, the *Top-K intersection* changes considerably. We further observe that by setting  $\beta$  too extreme, second gradients vanish, resulting in the IFIA attack not being able to find good adversarial inputs. This is illustrated in Figure 4, where the approximated second derivative is shown for several  $\beta$  values. Previous work has already hinted towards the dependency (Dombrowski et al. 2019) of robustness in attribution maps on  $\beta$ , however, the authors use the Softplus approximation for extracting the attribution maps as well, thus smoothing the curvature of the classifier. We are the first to only use this approximation for the second order gradients, hence keeping saliency maps unchanged and giving a better estimate for the true attribution robustness of ReLU networks.

Albeit reporting the aforementioned results and dependencies, we would like to stress the following points:

- Providing a fair comparison on the performance of robust attribution methods is not straightforward. Since second order gradients are irregular in DNNs, we emphasize the need for *detailed reporting* of the experimental setup.
- Methods may perform differently depending on data domains. We showed results for vision datasets, but in future research, evaluations on *other types of inputs* are crucial for a broad understanding of generalization capabilities for each method.
- We analyzed some parameters that influence the estimated

attribution robustness. However, an *extensive* and *systematic study* on more parameter dependencies is needed to provide a profound basis for developing and evaluating robust attributions in neural networks.

## Conclusion and Future Work

This work introduced a generalized notion of attributional robustness with the *framework for attributional robustness* (FAR) to provide objectives for increasing the robustness of attribution maps in DNNs. It allows direct optimization for robust attributions, with optionally coupling it to robust predictions. We showed how current existing objectives can be concretized from this framework. Moreover, we provided novel instantiations of FAR, AAT and AdvAAT, methods that directly optimize for high correlation of attributions for similar inputs as well as robust predictions. They perform comparably or better than current state-of-the-art methods, while generalizing to any saliency algorithm, without assumptions on the nature of the input data. Finally, we identified parameter dependencies of robust attributions that necessitate careful assessment of methods on their dependencies on these parameters.

This work opens up many interesting directions for future research. First, the assessment of **additional training parameters** that influence attribution robustness would be crucial. We plan to address this topic by extensive experiments on a diverse set of data in many domains. This could potentially lead to a better understanding of the connection between robust saliency maps and interpretability. Second, since our framework allows for robust training on any attribution map, we are particularly interested in assessing the robustness of **non-differentiable maps** like Occlusion (Zeiler and Fergus 2014). Prerequisite are **gradient estimates** for these attribution maps, which are another direction of future research. On a slightly different note, exploring the *connection between robust predictions and robust attributions* might lead to additional insights into the decision process of neural networks.

## References

- Chen, J.; Wu, X.; Rastogi, V.; Liang, Y.; and Jha, S. 2019. Robust Attribution Regularization. In *Advances in Neural Information Processing Systems*, 14300–14310.
- Dombrowski, A.-K.; Alber, M.; Anders, C.; Ackermann, M.; Müller, K.-R.; and Kessel, P. 2019. Explanations can be manipulated and geometry is to blame. In *Advances in Neural Information Processing Systems*, 13589–13600.
- Etmann, C.; Lunz, S.; Maass, P.; and Schönlieb, C.-B. 2019. On the Connection Between Adversarial Robustness and Saliency Map Interpretability. *arXiv preprint arXiv:1905.04172*.
- Ghorbani, A.; Abid, A.; and Zou, J. 2019. Interpretation of Neural Networks is Fragile. In *Proceedings of the AAAI Conference on Artificial Intelligence*, volume 33, 3681–3688.
- Glorot, X.; and Bengio, Y. 2010. Understanding the difficulty of training deep feedforward neural networks. In *Pro-*

*ceedings of the Thirteenth International Conference on Artificial Intelligence and Statistics*, 249–256.

He, K.; Zhang, X.; Ren, S.; and Sun, J. 2015. Surpassing Human-Level Performance on ImageNet Classification. In *Proceedings of the IEEE International Conference on Computer Vision*, 1026–1034.

He, K.; Zhang, X.; Ren, S.; and Sun, J. 2016. Deep Residual Learning for Image Recognition. In *Proceedings of the IEEE Conference on Computer Vision and Pattern Recognition*, 770–778.

Kendall, M. G. 1938. A new measure of rank correlation. *Biometrika* 30(1/2): 81–93.

Krizhevsky, A. 2009. Learning Multiple Layers of Features from Tiny Images. Technical report, Department of Computer Science, University of Toronto.

LeCun, Y. 1998. The MNIST database of handwritten digits. <http://yann.lecun.com/exdb/mnist/> .

Madry, A.; Makelov, A.; Schmidt, L.; Tsipras, D.; and Vladu, A. 2017. Towards Deep Learning Models Resistant to Adversarial Attacks. *arXiv preprint arXiv:1706.06083* .

Paszke, A.; Gross, S.; Massa, F.; Lerer, A.; Bradbury, J.; Chanan, G.; Killeen, T.; Lin, Z.; Gimelshein, N.; Antiga, L.; et al. 2019. Pytorch: An Imperative Style, High-Performance Deep Learning Library. In *Advances in Neural Information Processing Systems*, 8026–8037.

Pearson, K. 1895. Notes on Regression and Inheritance in the Case of Two Parents. *Proceedings of the Royal Society of London* 58(347-352): 240–242.

Shrikumar, A.; Greenside, P.; and Kundaje, A. 2017. Learning Important Features Through Propagating Activation Differences. *arXiv preprint arXiv:1704.02685* .

Simonyan, K.; Vedaldi, A.; and Zisserman, A. 2013. Deep Inside Convolutional Networks: Visualising Image Classification Models and Saliency Maps. *arXiv preprint arXiv:1312.6034* .

Singh, M.; Kumari, N.; Mangla, P.; Sinha, A.; Balasubramanian, V. N.; and Krishnamurthy, B. 2019. On the Benefits of Attributional Robustness. *arXiv preprint arXiv:1911.13073* .

Smilkov, D.; Thorat, N.; Kim, B.; Viégas, F.; and Wattenberg, M. 2017. SmoothGrad: removing noise by adding noise. *arXiv preprint arXiv:1706.03825* .

Stallkamp, J.; Schlipsing, M.; Salmen, J.; and Igel, C. 2011. The German Traffic Sign Recognition Benchmark: a multi-class classification competition. In *The 2011 International Joint Conference on Neural Networks*, 1453–1460. IEEE.

Sundararajan, M.; Taly, A.; and Yan, Q. 2017. Axiomatic Attribution for Deep Networks. In *Proceedings of the 34th International Conference on Machine Learning*, volume 70, 3319–3328.

Wang, Z.; Wang, H.; Ramkumar, S.; Fredrikson, M.; Mardziel, P.; and Datta, A. 2020. Smoothed Geometry for Robust Attribution. *arXiv preprint arXiv:2006.06643* .

Xiao, H.; Rasul, K.; and Vollgraf, R. 2017. Fashion-MNIST: a Novel Image Dataset for Benchmarking Machine Learning Algorithms. *arXiv preprint arXiv:1708.07747* .

Zeiler, M.; and Fergus, R. 2014. Visualizing and Understanding Convolutional Networks. In *European Conference on Computer Vision*, 818–833. Springer.

## Technical Appendix

**Training parameters and architectures.** We conduct experiments on four vision datasets (MNIST, Fashion-MNIST, CIFAR-10 and GTSRB) to compare our attributional robustness method to state-of-the-art algorithms. For each, we train separate DNN architectures that are detailed below. Each model is implemented in *PyTorch 1.3.1* and is trained distributedly on four NVIDIA Tesla P100 GPUs with the PyTorch Distributed Data Parallel wrapper. We fix all seeds to 42.

The adversarial accuracy ( $\mathbb{A}$ ) of the models is determined by the PGD attack, run for 40 iterations and 3 random restarts. We define a relative step of  $1.2/40$  for this attack. The  $\epsilon$ -bounds vary on each model and are detailed in the next paragraphs. We determine the attributional robustness ( $\mathbb{I}_N$  and  $\mathbb{C}_O$ ) of each model with the *iterative feature importance attack* (IFIA), executed for 7 iterations using their *Sum-of-Top-K* dissimilarity function. We report the lowest resulting robustness of the Integrated Gradients (IG) - estimated with 5 steps - on 3 random restarts. The relative step size used IFIA is  $1.2/7$ . If not indicated otherwise, we use a  $\beta$ -value of 1.0 in the second order ReLU gradient approximation. We use the default PyTorch weight initializations for each model.

### MNIST.

*Architecture and data.* We train a CNN with two convolutions of size 32 and 64 respectively, followed by ReLU activations and  $2 \times 2$  pooling layers. The activations are then flattened and a 1024-sized fully connected layer is appended. We use data normalization with means (0.1307,) and standard deviations (0.3081,) before feeding the data into the network.

*Evaluation.* We use an adversarial bound of 0.3 for estimating both adversarial and attributional robustness. We use  $k=100$  for estimating  $\mathbb{I}_N$ .

*Natural model.* For training the natural model, we use the Adam optimizer with a learning rate of 0.0001 and a batch size of 50. We train for 100 epochs over the whole dataset.

*Adversarial model.* To train the adversarial MNIST model we use the Adam optimizer with a learning rate of 0.0001 and a batch size of 50. During each update, we apply the PGD attack for 7 iterations with a relative step size of  $1.2/7$ , with random start to determine the adversarial images. We use a ratio of 0.7 of adversarial examples in each batch and train for 200 epochs, keeping the batch size 50.

*Align model.* We train the Align model with the Adam optimizer with a learning rate of 0.0001 for 150 epochs, with a batch size of 50. We set the regularization parameter  $\lambda$  to 0.5, adapt the IFIA attack to maximize the Alignment triplet loss, set the relative step size to  $1.2/7$ , and use random start in the attack to solve the inner maximization.

*AAT and AdvAAT model.* We train both models with the Adam optimizer and learning rate 0.0001 for 150 and 250 epochs respectively, with a batch size of 50. The regularization parameters  $\lambda$  and  $\gamma$  are set to 0.5 both, and we use IFIA attack with a relative step size of  $1.2/7$ , with random start, on IG to solve the inner maximization. During training, we use the *Sum-of-Top-K* dissimilarity with  $k=100$ .

### Fashion-MNIST.

*Architecture and data.* We use the same architecture for Fashion-MNIST as for MNIST.

*Evaluation.* We use an adversarial bound of 0.1 for estimating both adversarial and attributional robustness. We use  $k=100$  for estimating  $\mathbb{I}_N$ .

*Natural model.* For training the natural model, we use the Adam optimizer with a learning rate of 0.0001 and a batch size of 50. We train the model for 100 epochs over the whole dataset.

*Adversarial model.* To train the adversarial model, we use the Adam optimizer with a learning rate of 0.0001. We set the batch size to 50. During each update, we apply the PGD attack for 7 iterations with a relative step size of  $1.2/7$ , with random start to determine the adversarial images. We use a ratio of 0.7 of adversarial examples in each batch and train for 200 epochs.

*Align model.* We train the Align model with the Adam optimizer with a learning rate of 0.0001 for 200 epochs, with a batch size of 50. We set the regularization parameter  $\lambda$  to 0.5, attack the Alignment with IFIA with a relative step size of  $1.2/7$ , with random start, to solve the inner maximization.

*AAT and AdvAAT model.* We train both models with the Adam optimizer and learning rate 0.0001 for 150 and 250 epochs respectively, using a batch size of 50. We set the regularization parameters  $\lambda$  and  $\gamma$  to 0.5 both, and use IFIA attack with a relative step size of  $1.2/7$ , with random start, on IG to solve the inner maximization. During training, we use the *Sum-of-Top-K* dissimilarity with  $k=100$ .

### CIFAR-10.

*Architecture and data.* We train a WideResnet consisting of 3 layers for CIFAR-10 with 160, 320 and 640 planes respectively. Each layer comprises 4 blocks, with two convolutional and a shortcut layer. We use dropout in each block with a probability of 0.3 and omit batch normalization. The data is normalized with means (0.4914, 0.4822, 0.4465) and standard deviations (0.2023, 0.1994, 0.2010). We then apply color jitter and random affine transformations on the training dataset before feeding it into the classifier.

*Evaluation.* We use an adversarial bound of 0.03 for estimating both adversarial and attributional robustness. We use  $k=1000$  for estimating  $\mathbb{I}_N$ .

*Natural model.* We train the natural model with the Adam optimizer using a learning rate of 0.0001 and a batch size of 50. We train the model for 100 epochs.

*Adversarial model.* We use the Adam optimizer with a learning rate of 0.0001 to train the adversarial model. During each update, we apply the PGD attack for 7 iterations with a relative step size of  $1.2/7$ , with random start to determine the adversarial images. We use a ratio of 0.7 of adversarial examples in each batch and train for 150 epochs, utilizing a batch size of 50.

*AAT and AdvAAT model.* We train both models with the Adam optimizer and learning rate 0.0001 for 50 epochs, with a batch size of 20. We set the regularization parameters  $\lambda$  to 0.5 and  $\gamma$  to 0.2, and use IFIA attack with a relative step

size of 1.2/7, with random start, on IG to solve the inner maximization. During training, we use the *Sum-of-Top-K* dissimilarity with  $k=1000$ .

**GTSRB.**

*Architecture and data.* We use the same architecture for GTSRB as for CIFAR-10. We apply normalization to the data with means (0.3337, 0.3064, 0.3171) and standard deviations (0.2672, 0.2564, 0.2629). We apply color jitter and random affine transformations on the training dataset.

*Evaluation.* We use an adversarial bound of 0.03 for estimating both adversarial and attributional robustness. We use  $k=1000$  for estimating IN.

*Natural model.* For training the natural model, we use the Adam optimizer with a learning rate of 0.0001 and a batch size of 50. We train the model for 100 epochs over the whole dataset.

*AAT and AdvAAT model.* We train both models with the Adam optimizer and learning rate 0.0001 for 50 and 75 epochs respectively, using a batch size of 20. We set the regularization parameters  $\lambda$  to 0.5 and  $\gamma$  to 0.2 respectively, and use IFIA attack with a relative step size of 1.2/7, with random start, on IG to solve the inner maximization. During training, we use the *Sum-of-Top-K* dissimilarity with  $k=1000$ .

**Initialization methods.** We use seven different initialization methods for addressing the dependency of attributional robustness on the initialization. These are detailed in the next paragraphs. If a parameter is not mentioned, it is kept as the default value defined in PyTorch. The training setup is kept constant for each initialization, and corresponds to the setup mentioned in the previous section for the different models.

**PTD.** Default PyTorch initialization for linear and convolutional layers. This is the He uniform initialization with  $a = \sqrt{5}$  for the weights and a uniform initialization with bounds  $\pm b = \pm 1/\sqrt{\text{fan\_in}}$  for the bias terms.

**CUST.** Custom initialization method. Weights are initialized utilizing a zero-centered normal distribution with a standard deviation of 0.1, and biases are initialized to be 0.1, both for linear and convolutional layers.

**UNI.** Uniform initialization method. Weights and biases are initialized utilizing a uniform distribution with bounds  $\pm b = \pm 0.1$  for all layers.

**HU.** He uniform initialization method. Weights are initialized utilizing the default PyTorch He uniform initialization, biases are set to zero.

**HN.** He uniform initialization method. Weights are initialized utilizing the default PyTorch He normal initialization, biases are set to zero.

**GU.** Glorot uniform initialization method. Weights are initialized utilizing the default PyTorch Glorot uniform initialization, biases are set to zero.

**GN.** Glorot normal initialization method. Weights are initialized utilizing the default PyTorch Glorot normal initialization, biases are set to zero.

Init.	Model	NA	AA	IN	CO
PTD	Nat	99.1%	0.0%	0.23	0.20
	Adv	99.0%	93.9%	0.35	0.05
	AAT	98.9%	8.7%	0.39	0.28
CUST	Nat	98.8%	0.0%	0.09	0.03
	Adv	98.8%	88.9%	0.21	0.02
	AAT	98.6%	8.7%	0.30	0.18
UNI	Nat	99.2%	0.0%	0.18	0.13
	Adv	98.9%	93.6%	0.40	0.08
	AAT	98.7%	5.5%	0.33	0.24
HU	Nat	99.2%	0.0%	0.13	0.08
	Adv	99.0%	93.6%	0.12	0.01
	AAT	98.3%	7.2%	0.38	0.24
HN	Nat	99.2%	0.0%	0.10	0.06
	Adv	99.1%	93.6%	0.11	0.01
	AAT	98.5%	4.3%	0.36	0.24
GU	Nat	99.2%	0.0%	0.27	0.19
	Adv	99.0%	93.6%	0.21	0.45
	AAT	98.8%	6.4%	0.38	0.27
GN	Nat	99.2%	0.0%	0.26	0.20
	Adv	99.0%	94.0%	0.37	0.55
	AAT	98.7%	9.1%	0.39	0.28

Table 2: Estimated attributional robustness (IN and CO) for several different initialization methods (Init.). The results are reported for models trained naturally (Nat), adversarially (Adv) as well as with our AAT objective on MNIST. The natural and adversarial accuracy is given in the NA and AA columns. While accuracies of the models are similar, their estimated attributional robustness varies significantly throughout the initializations.